Late Accepted Papers

J. Synchrotron Rad. (1999). **6**, 800–802

'Atomic' XAFS as a probe of electronic structure

D. E. Ramaker and W. E. O'Grady

[a]*Department of Chemistry and Materials Science Institute, George Washington University, Washington, DC 20052, USA,* [b]*Chemistry Division, Naval Research Laboratory, Washington, DC 20375, USA*

Atomic XAFS (AXAFS) offers the potential for a new tool to gain relatively detailed electronic structure and polarization information on systems, *in-situ*, that may not contain long range geometric order. We have shown previously that AXAFS can monitor changes in the charge of less than 0.05e per surface Pt atom on a metallic cluster, and "sees" interactions from ions 2 and 3 shells removed from the absorber atom. The AXAFS lineshape allows a differentiation between the through space field polarization and the through bond inductive effects. Applications have been made to *in situ* Pt electrodes, ion-cation interactions in solution, and supported noble metal catalysts.

Keywords: EXAFS, Atomic XAFS, electrochemistry, zincate, ion-pair interactions

1. Introduction

The total absorption cross section is normally written $\mu = \mu_o(1+\chi)$. Upon absorbing an x-ray, the absorbing atom accounts for the major part μ_o of the absorption coefficient. The structure in χ enables the local geometry about the absorbing atom to be determined utilizing EXAFS (extended x-ray absorption fine structure) (Koningsberger & Prins, 1988). Holland et al (1978) and more recently Rehr et al (1994) noted that μ_o is not a totally smooth function, but can also have structure χ_a due to scattering from the periphery of the absorbing atom, i.e. $\mu_o = \mu_a(1+\chi_a)$ with μ_a the absorption cross section for the free atom in contrast to that for the embedded atom μ_o. This χ_a , called "atomic" XAFS [AXAFS] (Holland et al, 1978), offers the possibility to obtain electronic structure information utilizing a procedure comparable to EXAFS.

The AXAFS contribution is best reflected in the Fourier Transform (FT) of χ_a, which produces the first peak at approximately 1/2 the first shell bond-length. χ_a can be expressed approximately in a first distorted wave Born approximation (Rehr et al, 1994; Ramaker et al, 1998),

$$\chi_a \approx -(2m/(kh^2))\ \mathrm{Im} \int e^{2ikr+2i\delta}\ \Delta V\ dr, \qquad 1)$$

where the factor $\Delta V = V_e(r)-V_{tf}(r)$ is the difference between the potential of the embedded absorber atom $V_e(r)$, and the "truncated" free absorber atom, V_{tf}. Here $V_{tf}(r) = \min[V_{free}(r), V_{int}]$ where V_{free} is the free atom potential and V_{int} is the interstitial potential for the embedded atom in the muffin-tin approximation. If a phase corrected and k weighted Fourier transform of χ_a is taken (Ramaker et al, 1998), the result,

$$|\mathrm{FT}(ke^{-2i\delta}\chi_a)| \approx \Delta V^*\Gamma, \qquad 2)$$

indicates that the absolute magnitude of the FT is ΔV broadened by a function Γ. Thus the FT directly reflects the change in the potential of the absorber atom. More specifically, the FT can be represented by the area between V_{tf} and V_e and below V_{cut} ($V_{cut} = 2*V_{int} + |E_f|$) as illustrated in Fig. 1 (Ramaker et al, 1998), where E_f is the Fermi energy. From a more chemical point of view, the AXAFS contributions are caused by photoelectron scattering off of the localized deeper valence electrons pulled out to the periphery of the absorber atom.

2. Application to the zincate anion – hydrated metal cation pair interaction

Effects resulting from the presence of atoms two or more shells removed from the absorber are also visible. Both the near-edge and extended structure in the Zn K-edge XAS of $Zn(OH)_4^{2-}$ ions in basic solution reveal changes in the AXAFS features due to ion pair interactions with hydrated cations (Ramaker et al, 1999). By preparing solutions with different alkali metal cations, Li^+, Na^+, K^+, Rb^+, one can systematically vary the cation of the ion-pair interaction, and thus control the nature of the ions in the outer shells of the anion-cation complex (Ramaker et al, 1997). These data reveal that the AXAFS intensity varies significantly as a result of polarization of the zinc atom by the cation, without appreciably altering the

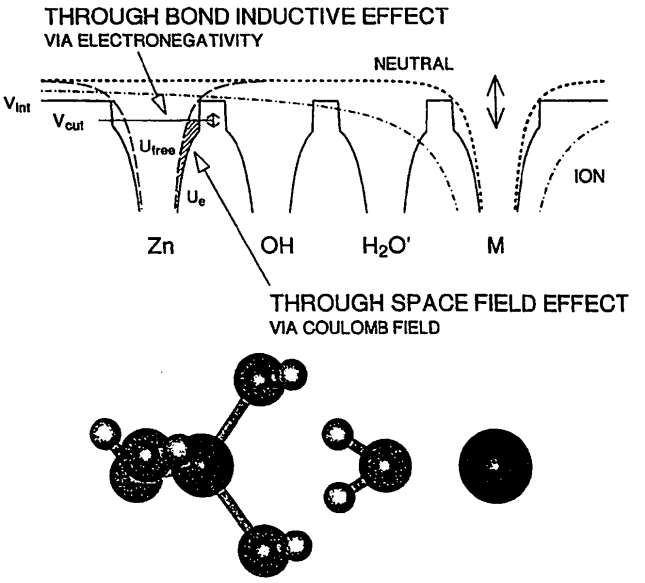

Fig. 1 Top) Schematic potential curves illustrating the "through bond inductive" and "through space field" effects. Shown are the neutral and ionic M potentials, the free and embedded absorber Zn potential, and the O (H) and $(H_2)O'$ potentials. The double arrows indicate that a large change in the M electronegativity (change in V_{int}) can cause a small change (small double arrow) in the overall V_{int} of the system.
Bottom) Schematic diagram of the zincate - hydrated M cluster with atoms defined as indicated above. Although these M ions typically have hydration numbers from 4-6, only the H_2O nearest the zincate ion is shown.

dominant first shell EXAFS contribution that results from scattering off the shell of OH ions around the Zn atom.

As illustrated in Fig. 1, the well-known muffin-tin approximation "clips" the exact potential at the muffin-tin radius R_{mt} and sets it equal to the interstitial potential V_{int} (Rehr et al, 1994; Ramaker et al, 1998). Inside R_{mt} the potential is assumed to be spherical, outside it is assumed to be flat and zero (i.e. no forces are exerted on the particle in the interstitial region). V_{int} is determined by averaging the potential of all the atoms in the cluster at R_{mt}, and this determines the zero of energy or the effective bottom of the itinerant band. In this muffin-tin model, polarization by neighboring atoms can modify the absorber atom in two different ways:

1) By the direct overlap of the nearby atom potentials, also referred to as the "through space field effect" (Reynolds, 1980), or
2) By affecting the average V_{int} and V_{cut}, which mimics the "through bond inductive effect" (Reynolds, 1980). This is true because if a neighboring atom is highly electronegative, V_{int} will be more negative, which means that more electrons will be delocalized into the interstitial region, exactly the nature of the inductive effect.

These two interactions are illustrated by the neutral and ion (long-range Coulomb) potentials of the cation on the Zn absorber atom in Fig. 1.

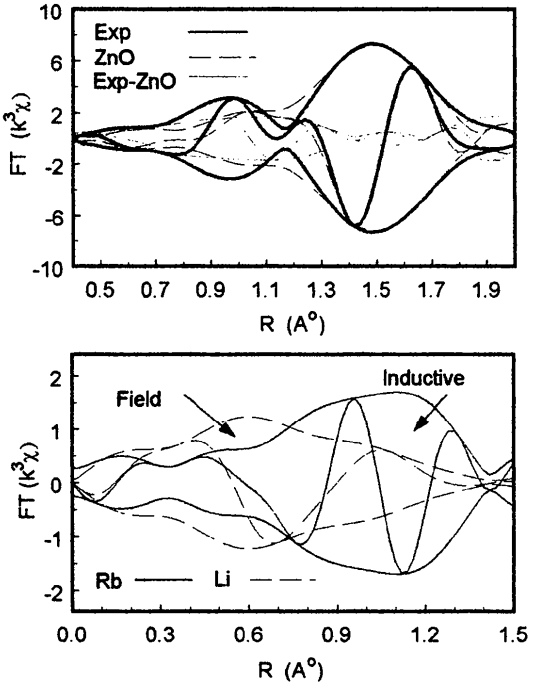

Fig. 2a) Fit of the Fourier Transform (k^3 weighting, Δk = 2.6-12 $Å^{-1}$) of the experimental χ with the FT of χ_{Zn-O} obtained from FEFF7 and fit to the experiment in the region R = 1.3-1.8Å. Also shown is the difference (χ-χ_{Zn-O}), which isolates the AXAFS and the higher multiple scattering contributions.

2b) Comparison of the extracted AXAFS (imaginary and amplitude of the FT) for both Li and Rb with the differences arising from the through-space field and through-bond inductive effects noted.

Figure 2a shows the FT (k = 2.6-12$Å^{-1}$) of the experimental χ (= χ+ χ_a) with contributions from the AXAFS around 1 Å, the EXAFS Zn-O single scattering around 1.5 Å and higher multiple scattering at still larger R. We used background removal criteria developed previously, (Ramaker et al, 1998) which reliably gives the magnitudes of the AXAFS. A significant overlap exists between the AXAFS and Zn-O single scattering. To isolate the AXAFS, the difference file technique (Kampers, 1995) was utilized. The necessary ZnO scattering parameters were calculated using FEFF7. Fig. 2a shows the fit to χ_{Zn-O} and the difference, χ-χ_{Zn-O}, which below R = 1.5 Å is essentially χ_{AXAFS}. Notice the significant interference between χ_{AXAFS} and χ_{Zn-O}, revealing the importance of the difference file technique to isolate χ_{AXAFS}. Utilizing the same technique for both Li and Rb, we compare the results in Fig. 2b.

The charged cation has a long range Coulomb potential which overlaps with the Zn atom 3 shells removed and lowers the embedded Zn atom potential relative to the free atom (the through space field effect, cf. Fig.1). This increases the AXAFS, and makes it larger for the Li case because of the smaller Zn-M distance for Li. However, the more electronegative Li cation brings down V_{cut} which reduces the AXAFS for Li compared with Rb (the through bond inductive effect, Fig. 1) in the larger R region or periphery of the Zn atom. Fig. 2b clearly reveals both effects, with the Li case having an increased intensity at low R, and much-reduced intensity at higher R.

Confirming evidence for the change in V_{int} between the Li and Rb complexes comes from the theoretical fit to the experimental χ_{Zn-O}. While the coordination number, n, (around 3.7), σ^2 (0.004) and R_{Zn-O} (1.95Å) parameters remained constant within estimated error, the ΔE_o parameter changed from 4.0 eV for Rb to -1 eV for Li, a change of 5 eV.

Fig. 2b indicates that in this ion-pair interaction, the through bond inductive effect is more important than the through space field effect. This is perhaps rather surprising considering that one of the bonds transmitting the inductive effect is a relatively weak hydrogen bond. However, the through space field effect should also be rather weak in a solvent with a dielectric constant as high as water, even though "bound" water is known to have a smaller dielectric constant than bulk water (Reynolds, 1980). In organic molecules, inductive effects have been observed to dominate only for very short distances between the probe and substituent atom (Reynolds, 1980) similar to the distances in this work.

3. Summary

The existence of AXAFS contributions in XAS is still somewhat controversial. It has been indicated that the near edge features in μ_o, at least in some systems, are not due to AXAFS, but are due to multi-electron excitations (Filiponi and DiCicco, 1996). However, the multi-electron excitations would not be expected to be sensitive to the cation interactions as seen here. Furthermore, we have recently shown that the AXAFS and multi-electron excitations in Pt foil can be individually isolated (van Dorssen Ramaker, & Koningsberger, 1999).

In other applications of AXAFS, we have shown recently that

1. AXAFS can monitor the charge on a metallic cluster with charges as small as 0.05e (electronic charge) (O'Grady et al, 1987).

2. The amplitude of the AXAFS directly correlates with the turn over frequency (TOF) for Pt clusters in zeolite LTL (i.e., the metal-support interaction is directly visible in the AXAFS) (Mojet et al,1998).
3. The inductive effect due to H adsorption on a supported Pt cluster is felt across the cluster and is highly dependent on the acidity of the support (Ramaker & Koningsberger, 1998).

We believe that AXAFS may offer a new tool to gain relatively detailed electronic structure and polarization information on systems, in situ; however, further theoretical development and understanding of the phenomenon is required. Such theoretical effort is appropriate, because XAS might have the possibility in the future to provide both geometric (from EXAFS) and electronic (from AXAFS) information from a single technique.

Support from the Office of Naval Research is gratefully acknowledged. The authors also gratefully acknowledge the support of the USDOE, Division of Materials Science, under contract no. DE-FG05-89ER45384 for its role in development and operation of beam line X11A at NSLS. Finally the authors acknowledge help with analysis of the data and stimulating discussions with D.C. Koningsberger.

References

Filiponi, A.& DiCicco A. (1996). Phys. Rev. **B53**, 9466-9467.

Holland, B.W. Pendry, J.B. Pettifer, R.F. & Bordas, J. (1978). J. Phys.C **11**, 633-642.

Kampers, F.W.H. (1988). EXAFS in catalysis, instrumentation and applications, Ph.D. Thesis, Technische Universiteit Eindhoven, Eindhoven Netherlands.

Koningsberger D.C. & Prins, R. (1988). *X-ray Absorption : Principles, Applications and Techniques of EXAFS, SEXAFS and XANES*, edited by Koningsberger D.C. and Prins, R., pp. 211-253, New York: John Wiley.

Mojet, B, Ramaker, D.E., Miller, J. & Koningsberger, D.C. (1998). To be published; Koningsberger, D.C. and Ramaker, D.E. (1999). This proceedings.

O'Grady, W.E., Qian, X. & Ramaker, D.E. (1997). J. Phys. Chem. **B101**, 5624-5626; O'Grady W.E. and Ramaker, D.E., (1998) Electrochemica Acta **44**, 1283-1287.

Ramaker, D.E., Qian, X., & O'Grady, W.E. (1999). Chem. Phys. Letters **299**, 221-226.

Ramaker, D.E., Qian, X., & O'Grady, W.E. (1997). J. Phys. IV France **7** C223-225; Qian, X., Sambe H., Ramaker, D.E. & O'Grady, W.E. (1998). Unpublished; Pandya, K.I. Russell, A.E. McBreen, J. & O'Grady, W.E. (1995). J. Phys. Chem. **99**, 11967-11973.

Ramaker, D.E., Mojet, B., Koningsberger, D.C.& O'Grady, W.E.(1998). J. Phys. Cond. Matter, **10** 8753-8766.

Ramaker, D.E. & Koningsberger, D.C. (1999). In preparation.

Rehr, J.J. Booth, C.H. Bridges, F. & Zabinsky, S.I. (1994). Phys. Rev. B **49**, 12347-12350.

Reynolds, W.F. (1980). J. Chem. Soc. Perkins II. 1980, 985-992.

van Dorssen, G.E., Ramaker, D.E. & Koningsberger, D.C. (1999), submitted to Phys. Rev. B.

(Received 10 August 1998; accepted 22 February 1999)